FIRST RESULTS FROM THE CHARA ARRAY. V. BINARY STAR ASTROMETRY: THE CASE OF 12 PERSEI

William G. Bagnuolo, Jr., Stuart F. Taylor, Harold A. McAlister, Theo ten Brummelaar, and Douglas R. Gies

Center for High Angular Resolution Astronomy and Department of Physics and Astronomy, Georgia State University,
Atlanta, GA 30303-3083; bagnuolo@chara.gsu.edu

Stephen T. Ridgway

National Optical Astronomy Observatory, 950 North Cherry Avenue, Tucson, AZ 85719; ridgway@noao.edu

Judit Sturmann, Laszlo Sturmann, Nils H. Turner, and David H. Berger

Center for High Angular Resolution Astronomy Array, Mount Wilson, CA 91023; judit@chara-array.org,
laszlo@chara-array.org, nils@chara-array.org, berger@chara-array.org

and

Donald Gudehus

Center for High Angular Resolution Astronomy, Georgia State University, Atlanta, GA 30303-3083; gudehus@chara-array.org

ABSTRACT

We have obtained high-resolution orbital data with the CHARA Array for the bright star 12 Persei, a resolved double-lined spectroscopic binary. We describe the data reduction process, which can give precision in separation of up to 25 μas along a given baseline. For this object we find a semimajor axis of $a = 53.18 \pm 0.15$ mas, which is 0.3% smaller than that of Barlow and coworkers, but with much improved precision. The inclination angle i increases to $128°17 \pm 0°14$, compared to $126°77 \pm 0°56$ of Barlow and coworkers, again with better precision. We also found an intensity ratio for the components in the K' band ($\lambda = 2.13$ μm) of $r = 0.72 \pm 0.01$, or $\Delta K' = 0.409 \pm 0.013$, after allowing for the partial resolution of the components. Assuming the spectral types of the components, we find that $\Delta V = 0.51$, as compared to 0.57 by Barlow and coworkers. The revised masses ($M_p = 1.382 \pm 0.019$ and $M_s = 1.240 \pm 0.017$ $M_\odot$) are found to be 5.8% larger than those of Barlow and coworkers, and the components are thus even more overmassive. The overall accuracy in the masses is about 1.3%, now primarily limited by the spectroscopically determined radial velocities. The precision of the masses due to the interferometrically derived "visual" orbit alone is only about 0.2%.

Key words: binaries: visual — instrumentation: high angular resolution — instrumentation: interferometers — stars: fundamental parameters — techniques: high angular resolution

1. INTRODUCTION

The star 12 Persei (HD 16739, HR 788) was originally discovered to be a double-lined spectroscopic binary by Campbell & Wright (1900) from plates from the Mills spectrograph at Lick Observatory. Since then there have been a series of improved measurements in both spatial ("visual") and spectroscopic data. The first orbital elements by Colacevich (1935, 1941) were from 26 Lick plates on which the double lines were clearly resolved. The system was found to be highly eccentric ($e = 0.67$), with a period of 331.0 days. McAlister (1978) used six speckle interferometry observations to obtain the inclination angle ($i = 123°0 \pm 2°0$), semimajor axis ($a = 57 \pm 3$ mas), and masses of the components, assuming the previous spectroscopic results. Additional speckle observations were listed by Hartkopf et al. (1997). More recently, the spectroscopic data were improved by Barlow et al. (1998; hereafter BSF98), who also revised the three-dimensional orbit and obtained masses for the components. The available data were summarized by Pourbaix (2000). Because long-baseline interferometry can provide 1–2 orders of magnitude better spatial precision than speckle interferometry, we thought it would be useful to revisit this system with the Center for High Angular Resolution Astronomy (CHARA) Array with the aim of improving the precision of the masses and obtaining an intensity ratio in the K' (2.13 μm) band.

2. OBSERVATIONS AND DATA REDUCTION

Observations of 12 Per, as summarized in Tables 1 and 2, were obtained at the CHARA Array, a six-element optical/IR interferometric array located on Mount Wilson, California (ten Brummelaar et al. 2005). At the longer baselines of the CHARA Array, 12 Per is overresolved in the sense that the fringe packets corresponding to the individual components do not overlap. Under normal fringe-scanning procedures, each scan shows dual fringe packets, such as those shown in Figure 1. For angular separation projected onto the baseline in the range of approximately 10–120 mas, nominal observing practice reveals separated fringe packets. In the relatively uncommon instance of a triple system consisting of a "wide" component in this range of separations orbiting a closer, shorter period pair, the wide component can serve as a nearly ideal calibrator star for the standard interferometric visibility analysis of a binary that calls for the target star being bracketed in a sequence of calibrators by a nearby calibrator. Similarly, a separated fringe packet binary may provide the opportunity for one component to calibrate the diameter determination of the other, as in the case of a system consisting of an early-type dwarf and a late-type giant.

In the present case, we ignore the visibility calibration process and use the separated fringe packets purely for astrometric purposes. This approach was first tried by Dyck et al. (1995) and has recently been refined to produce very high precision astrometry by Lane & Muterspaugh (2004) for binaries significantly wider than 12 Per. The latter work exploits the dual-star, narrow-angle astrometric capability of the Palomar Testbed Interferometer (PTI), which is equipped with dual delay lines on each arm. The PTI observations have attained night-to-night repeatability of 16 μas, capable of detecting sub-Jupiter-mass planets

TABLE 1
ORBITAL PARAMETER FITS

Parameter	All	$a + i$	BSF98
P....................	330.98199	330.98209	330.98209
T_0..................	1993.3396	1993.3395	1993.3395
e....................	0.658199	0.65740	0.657400
a....................	53.1774	53.18000	53.38000
i	128.1467	128.1700	126.7700
ω....................	49.00628	49.2900	49.2900
Ω....................	269.25574	269.2900	269.290
SSE...............	0.0029284	0.0034665	1.21136

orbiting one component of a nearby close visual (or speckle) binary. The CHARA Array was not intended as an astrometric instrument and lacks the narrow-angle capability of the PTI. Nevertheless, for stars like 12 Per, we show that we can achieve an internal precision of 25 μas.

Individually resolved fringe packets of binary stars are produced by scans at the CHARA Array with the "CHARA Classic" setup, using a piezoelectric (PZT) stack to modulate the optical path difference (OPD) by up to 170 μm. Each scan takes about 250 ms, and modulation goes both ways in a triangle wave. The filter setup is the K' band (2.13 μm). Up to 15 sets of 400 scans each can be collected in an hour.

We use three programs to reduce the data. The first produces a stack of scans sampled at 0.1 μm after using a notch filter around the scan frequency as described by McAlister et al. (2005). The program then determines the envelope of the packets by suppressing the negative spatial frequencies (T. A. ten Brummelaar 2003, private communication) and finally finds the locations of the packets with a seven-point parabolic fit around the two maxima. Figure 2 shows two consecutive scans for which the packet locations have been found.

The second program analyzes these data in terms of separations at discrete times. It begins by plotting the observed separations versus those predicted from the existing orbit, given the times. Figure 3 shows an example. Note that the separations are the positions of the PZT stack; the OPDs are twice this. For systems with packet separations of less than about 60 μm (roughly 100 mas on the sky) the measured separation is modulated periodically by the secondary star's packet riding over the sidelobes of the primary. The apparent position of the secondary packet is pulled slightly toward the position of the sidelobe of the primary (to a lesser extent, the position of the primary packet is also affected). We thus have a "free" phase reference without additional instrumentation. The second program does a five-parameter linear plus sinusoidal fit to the data. Figure 4 shows the data for the observations on 2004 September 28. These results are summarized as five separations versus time points at which the sinusoid term is zero (i.e., the crossing points of the sinusoid on the straight trend

TABLE 2
OBSERVATION PARAMETERS

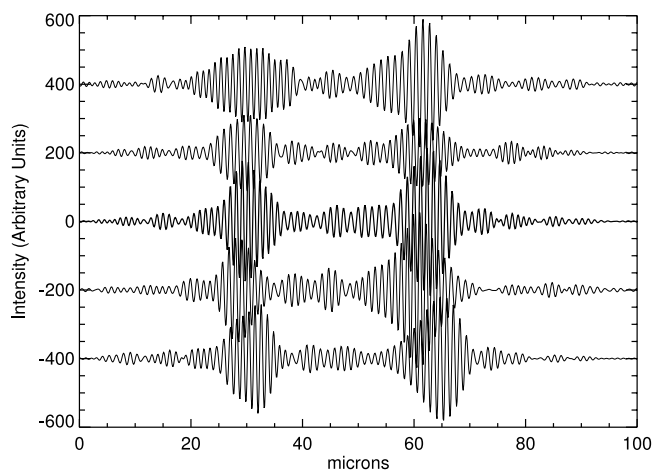| Date	t_1	t_2	n_f	n_l	Baseline
2003 Oct 9	8.124	8.942	1000	1	S2-W1
2004 Sep 23............	9.391	9.946	1194	3	S1-W1
2004 Sep 24............	9.044	9.480	1199	3	S1-W1
2004 Sep 28............	8.719	9.596	2384	5	S1-W1
2004 Nov 16...........	6.711	7.350	458	3	E1-W1
2004 Nov 18...........	7.102	7.434	1013	1	E1-W1
2004 Nov 30...........	5.643	6.645	3208	5	E1-W1

FIG. 1.—Five consecutive fringe scans of 12 Per, after filtering.

line). These times are determined by an interpolation from the predicted separations (x-axis). In addition to these "linear" fits, we can also exploit the "sidelobe verniering" effect to get more accuracy. To do this, we assign the closest $\lambda/2$ OPD ($\lambda/4$ in PZT distance) to the crossing points. We assume here that for an integral separation of $\lambda/2$ in OPD there is no bias in the separation of the peaks of the two packets due to overlapping sidelobes. For example, the predicted separations for 2004 September 23 are 33.1105, 33.6040, and 34.0976 μm at the three crossing points. The linear separations are significantly larger, at 33.9625, 34.5246, and 35.0866. The corresponding vernier separations are slightly larger (for this night) at 34.0800, 34.6125, and 35.1450. We discuss several estimates of the errors of these fits below. The (systematic) measurement errors due to the PZT stack itself are estimated to be about 0.1%. The errors in center wavelength, adopted as 2.130 μm from the measured transmission of the filter at LN2 temperatures, are probably greater. A comparison of the separations given by the linear and vernier fits for the three best nights in terms of seeing, 2004 September 23, 24, and 28, yielded a ratio of vernier-to-linear separations of 0.9971, which indicates that a wavelength should be 2.136 μm. This would increase the results for the semimajor axis given below by 0.27% or the masses by 0.8% (still considerably less than our [random] errors of 1.3%).

The third program takes the sets of separations produced by the second program for a set of nights and fits the best orbit on a grid of values of a (semimajor axis) and i (inclination angle). We
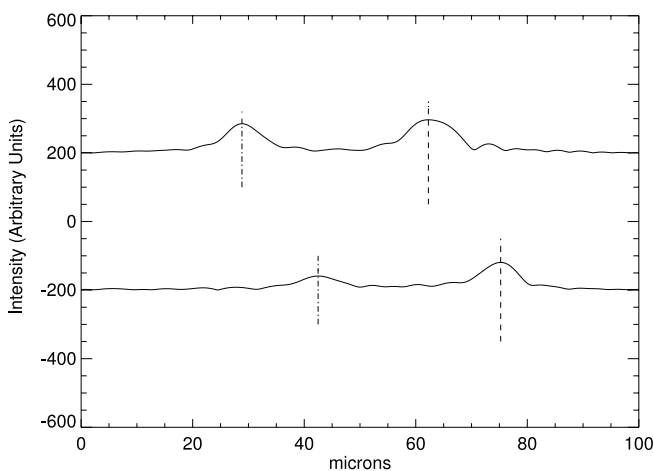

FIG. 2.—Two consecutive envelopes of fringe scans, after finding the packet maxima.
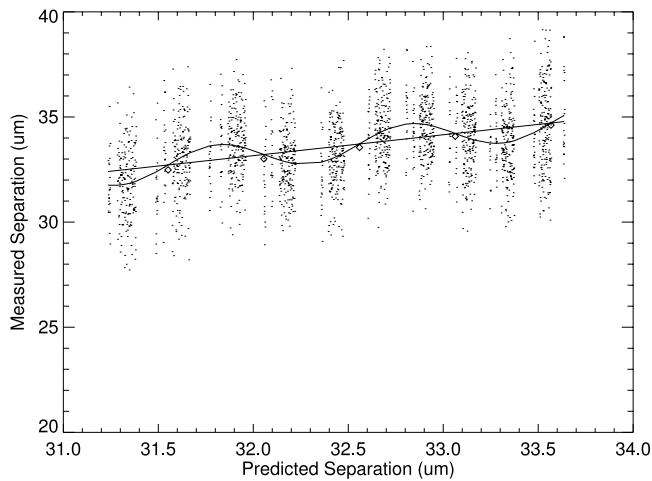
Fig. 3.—Observed vs. predicted 12 Per separations for the observations of 2004 September 28. The 2384 good data points are fitted with a five-parameter linear-sine fit. Diamonds indicate the vernier fit at the points where the sinusoid intersects the line.

chose this technique because the other parameters are well established by spectroscopy and prior speckle observations.

3. ORBIT RESULTS

Figure 5 shows the result from all seven observation nights, where the dotted line represents the revised orbit. The revised orbit shows an inclination $i = 128°.17$, about $2°$ more than the BSF98 value (i.e., a flatter angle toward the observer), but a semi-major axis only slightly less, $a = 53.18$ versus 53.38 mas from BSF98, and in close agreement with that of Pourbaix (2000). The explanation for this is simple: in the greatest separation cases (2003 December 5; 2004 September 23, 24, and 28) the measured
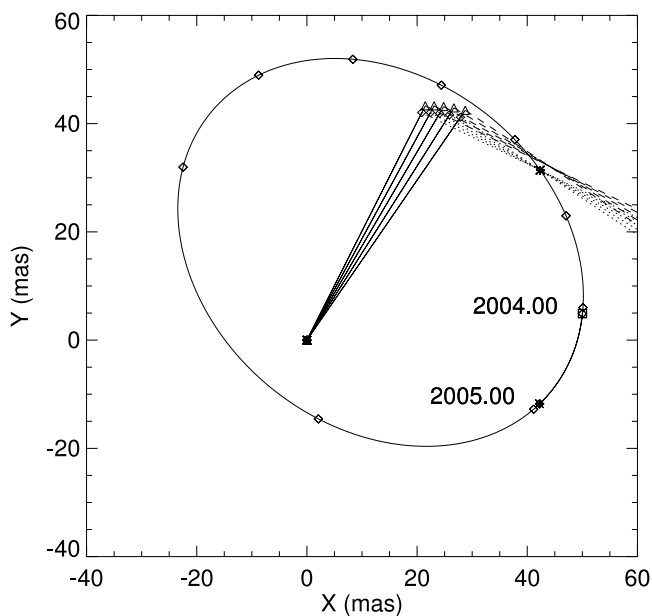

Fig. 4.—12 Per separations for 2004 September 28. The standard orbit of BSF98 is plotted between JY 2004.0 and 2005.0 with intervals of 0.1 yr (*diamonds*). Note that since the period is slightly shorter than a year, there is an overlap area. There are five separation points generated by the fit (*triangles*). The projected separations are shown by the dotted and dashed lines. For comparison, the five points at the same times for the BSF98 orbit are also shown. Note that these intersect the standard orbit point (*asterisk*). The observed separation points show a location outside the standard orbit.
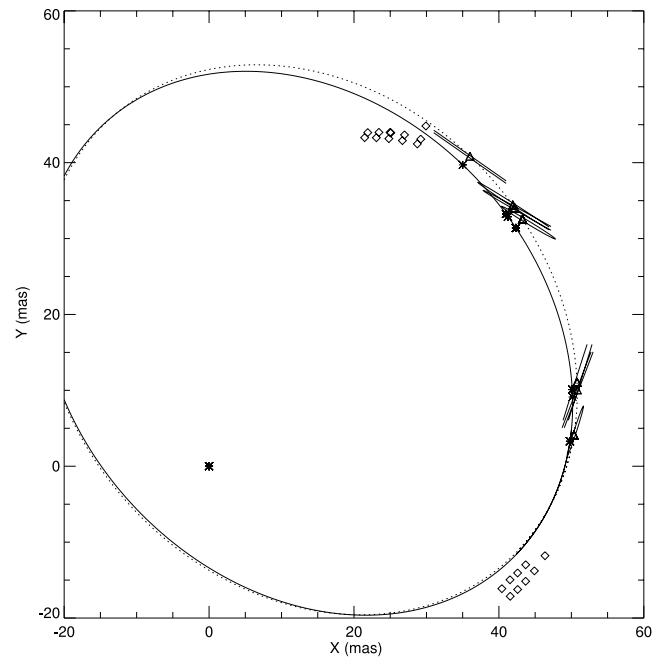

Fig. 5.—12 Per separations for all seven nights. The solid line represents the BSF98 orbit, and asterisks represent the standard locations during the nights. The dotted line represents the new orbit fit to the data, and the triangles represent the new orbit locations on the observing nights. The diamonds represent all the projected separations (21) derived from the seven nights. The error ellipses are plotted for each night's observation, as described in the text.

separation increases as the inclination angle flattens. But for observations near the line of nodes (e.g., 2004 November 30) the measured separation a is unchanged. Figure 6 plots the uncertainty in the determination of a and i. Note that a linear combination of the variables $(1.05a + i)$ is the major axis of the ellipse, and that quantity is much better determined than either a or i, which (fortunately) leads to a better determination of the masses.
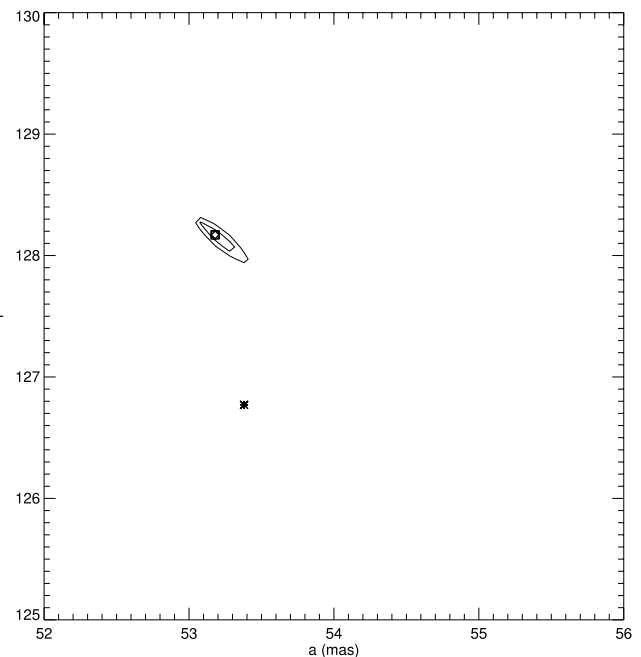

Fig. 6.—Orbital parameter fits in (a, i) for 12 Per. The asterisk indicates the parameters for the BSF98 orbit. Contours show 1σ intervals for the fits in (a, i) for the interferometric data (this paper).

We have made several estimates of the errors of these techniques. First, we made a series of simulations in which 200 sets of 2000 randomly generated data points with a "separation" varying from 30 to 32 μm were used. This corresponds to about 30 minutes of data. The amplitudes of the vernier wave and Gaussian random noise were set at 0.75 and 2.5 μm, respectively, which corresponds to what empirically was found to be "good" seeing ($r_0 = 10$ cm). The errors for linear and vernier fits were 127 and 32 nm, respectively, corresponding to 190 and 48 μas, respectively, for our longest baseline. For comparison, for 1 hr of data, the precisions are 134 and 34 μas.

Second, we can compare the data from three closely spaced nights, 2004 September 23, 24, and 28, during which good, but not exceptional, seeing prevailed (i.e., $r_0 \approx 8-11$ cm). For comparison we choose the value of the linear and vernier separation at the same predicted separation $x = 33.0$ μm. The linear fits for 2004 September 23, 24, and 28 were 33.7992, 34.0167, and 34.0841 μm, respectively. This produces a difference of 218 nm between September 23 and 24 and a difference of the average of September 23–24 and September 28 of 176 nm. The corresponding vernier fits for 2004 September 23, 24, and 28 at $x = 33.0$ μm were 33.8947, 33.8842, and 33.9556, respectively, for a difference of 10 nm between September 23 and 24 and a difference of the average of September 23–24 and September 28 of 66 nm. Third, we can use the overall $O - C$ fit data to the fitted orbit. The estimated standard error per 1000 scans for the 21 "lines" is 42 μas on the sky. (The unweighted median fit is 45 μas.)

We have also tried a more sophisticated analysis, using a Monte Carlo simulation in which we allow all seven parameters, not only a and i, to vary within the errors of BSF98. The best fit out of 10,000 trials yielded a modest improvement in the sum of squared errors (SSE) of 0.002928 versus 0.003467, where a and i vary alone. Table 1 shows the resulting parameter fits. It turns out that the fits for a and i with this technique are insignificantly different from the "a and i only" grid fit (53.177 mas and 128°.147 versus 53.18 mas and 128°.17, respectively). A slight change in the other parameters provided a slightly better fit. Table 2 summarizes some observational parameters for the seven nights. The columns give the data, the start and stop times of the observations (t_1 and t_2) in hours, and the number of good fringes and vernier lines (n_f and n_l, respectively).

4. INTENSITY RESULTS

Unlike single visibility measurements, separated fringe packets can also yield a direct estimate of the intensity ratio of the stars, as well as resolving the 180° ambiguity of the visibilities. The fraction of light in the secondary component, f, is given by $r/(1 + r)$, where r is the intensity ratio. Figure 7 shows a histogram of the intensity fraction for the 2004 September 28 data, which yields an estimated intensity ratio of 0.722. (The error in standard deviation in f of the 2180 histogram points is 0.08358, for a nominal error of 0.00179 in f, or 0.0053 in r.) Outliers in separation are first removed, as in the programs described above. A weighted sum for the five last nights gives an overall estimate of 0.716, which we round to 0.72 ± 0.01.

There are several sources of error in this process. The first is a sinusoidal variation in intensity ratio due to the same effect as sidelobe verniering. This is small and can be removed. Second, and much more important, is a correction for the partial resolution of the stars, which lowers the amplitudes of the packets (i.e., visibility). We can correct for partial resolution as follows: BSF98 give a parallax of 0.04224, $r_1 = 1.58$, $r_2 = 1.37$ (solar units), or diameters on the sky of 0.614 and 0.532 mas. For a baseline of 279 m, this yields, assuming the standard visibility
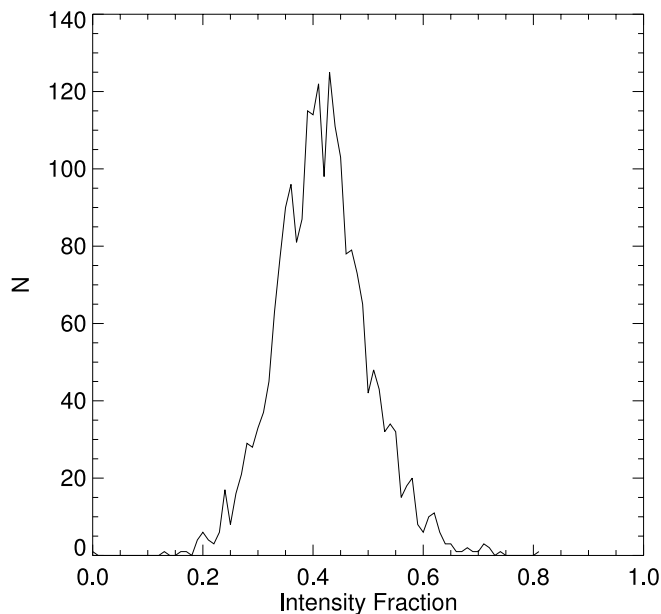

Fig. 7.—Histogram of intensity fractions for 2004 September 28 observations.

function for a uniform disk, visibilities of 0.827 and 0.868, for a ratio of 1.050. Thus, the true intensity should be 0.686, or $\Delta K' = 0.41$. According to the estimated interpolated spectral types of BSF98 (F8 V and G1.5 V), the magnitude difference in V of the stars is $\Delta V = 0.51$. This compares to the latter's estimate of $\Delta V = 0.57$ (with much worse precision).

From our new determination of the intensity ratio in the K' band, we find $\Delta K' = 0.409 \pm 0.013$ mag, which, when combined with the Two Micron All Sky Survey (2MASS) K magnitude, yields individual magnitudes of $K'_p = +4.45 \pm 0.29$ and $K'_s = +4.86 \pm 0.29$, with our relatively high level of photometric accuracy swamped by the poorly determined 2MASS magnitude.

5. DISCUSSION

Our determination of the angular semimajor axis is in excellent agreement with the BSF98 value while reducing the error by a factor of 3.5. Our value for the inclination angle i has increased to $128°.17 \pm 0°.14$. When these values of a and i are combined with the linear semimajor axis as determined by the elements P, e, k_p, and k_s, we obtain a new orbital parallax of 41.19 ± 0.21 mas, equivalent to a distance of 24.26 ± 0.12 pc, in comparison with the *Hipparcos* distance of 24.68 ± 0.76 pc (Perryman et al. 1997). This in turn leads to a mass sum of 2.622 ± 0.034 $M_{\odot}$ and, after incorporating the mass ratio from the velocity amplitudes, individual masses of $M_p = 1.382 \pm 0.019$ and $M_s = 1.240 \pm 0.017$. The gain in accuracy (but less than the factor of 3.5 improvement in a) over the BSF98 mass values demonstrates that the limiting factor in these determinations now lies in the accuracy of the velocity amplitudes. Moreover, the linear correlation in the astrometry of a and i (Fig. 6) noted above means that the mass estimate is better determined than either a or i because the masses are proportional to $a^3/\sin^3 i$. Random errors in the masses due to astrometry *alone* are thus only about 0.2%.

The masses of the stars are thus 5.8% greater than those found by BSF98, with an accuracy of 1.3%. Further improvements in spectroscopy could push the accuracy below the 1% level. This would require improving the existing accuracies of 500 m s^{-1} in BSF98 to 300 m s^{-1}, which seems possible given the stars'

projected rotational velocities of 5–6 km s^{-1}. Another avenue to be followed up spectroscopically is an improved abundance analysis, because as BSF98 noted, increasing the metal abundance would make the components lie closer to the zero-age main sequence and thus appear younger, given their masses.

6. CONCLUSIONS

We have shown that separated packet techniques with long-baseline interferometry produce good precision and repeatable results as applied to binary stars' separation and intensity ratios. The star HD 16739, or 12 Persei, following the discussion in BSF98, is still overmassive—in fact, 6% more overmassive—with better precision (about 1.3% in mass, one of a small number with this precision). We also have obtained a better intensity ratio in K', which corresponds to a magnitude difference of 0.409 ± 0.013, which translates to 0.51 in V, given the interpolated spectral types of BSF98. This is smaller than the value of 0.57 of BSF98, either because the estimate of the latter is mistaken or because the difference in subtypes between the stars is slightly greater than their estimate (F8 V and G1.5 V).

REFERENCES

Barlow, D. J., Scarfe, C. D., & Fekel, F. C. 1998, AJ, 115, 2555 (BSF98)
Campbell, W. W., & Wright, W. H. 1900, ApJ, 12, 254
Colacevich, A. 1935, PASP, 47, 284
———. 1941, Oss. Mem. R. Oss. Astrofis. Arcetri, 59, 15
Dyck, H. M., Benson, J. A., & Schleorb, F. P. 1995, AJ, 110, 1433
Hartkopf, W. I., McAlister, H. A., & Mason, B. D. 1997, Third Catalog of Interferometric Measurements of Binary Stars (CHARA Contrib. 4; Atlanta: Georgia State Univ.)
Lane, B. F., & Muterspaugh, M. W. 2004, ApJ, 601, 1129
McAlister, H. A. 1978, ApJ, 223, 526
McAlister, H. A., et al. 2005, ApJ, 628, 439
Perryman, M. A. C., et al. 1997, A&A, 323, L49
Pourbaix, D. 2000, A&AS, 145, 215
ten Brummelaar, T. A., et al. 2005, ApJ, 628, 453